



Radiation Dose Optimization for Contrast-Free Adult Skull CT Protocol

F. N. Torres¹ , J. V. Real^{1,2} , and A. M. Malthez¹ 

¹ Curitiba, Brazil

flavianasctorres@gmail.com

² Clinic Hospital Complex of Federal University of Parana, Curitiba, Brazil

Abstract. Among all radiological techniques, computed tomography delivers the highest radiation dose to the patient. Aiming for the radiological protection of those, this project set out to optimize the Contrast-free adult skull protocol of the Clinic Hospital Complex of the Federal University of Parana. Four different suggested protocols were submitted to quality control tests to analyze whether it was possible to reduce the dose without a significant loss in the image quality and decide, among those, which one could be implemented at the hospital. Two out of the four suggestions obtained satisfactory results.

Keywords: Radiation dose · Computed tomography · Imaging diagnosis · Dose optimization

1 Introduction

Developed by Godfrey Hounsfield in the sixties, Computed Tomography (CT) has the same basic principles as conventional radiography, a method through which images are acquired by exposing a medium to x-rays. The CT scan contains an x-ray tube located inside a gantry, which rotates 360° around the patient's table and obtains 'sliced' high-quality images of the irradiated structure [1].

Due to its high-definition images, CT has become an indispensable tool in radiodiagnostics. Therefore, international radiation protection institutions, such as the International Commission on Radiation Protection (ICRP), the American Association of Physicists in Medicine (AAPM) and International Atomic Energy Agency (IAEA), established recommendations for both imaging quality assurance and dose optimization, which consists of procedures specifically created to maintain a high diagnostic and treatment quality for the patients [2–4]. The Brazilian body responsible for regulatory in image diagnosis, ANVISA (*Agência Nacional de Vigilância Sanitária*), established in the current resolution the quality assurance tests in at RDC 611, and IN 93 regarding CT's quality assurance [5, 6]. Therefore, there is not a Brazilian technical document that described the methodology to run the tests. In this case, international documents and protocols can be adopted, as the IAEA N19 recommendations [4].

Although there is no limit value for medical exposure, the radiological protection of patients during diagnostic procedures should be improved, keeping the radiation dose as

low as it can be to obtain an image good enough for diagnosis and treatments. Thus, the need arises to search for ways to optimize the patient's radiation dose, especially in CT exams - which has one of the highest rates of exposure in medical imaging -, not only to improve image quality but also to prevent patient exposure as much as possible [7].

Therefore, the main goal of this article was to optimize the Contrast-free adult skull protocol, retaining (or improving) the image quality for clinical diagnosis, whilst also reducing the patient's absorbed dose in CT examinations at the Clinic Hospital Complex of the Federal University of Parana (CHC-UFPR). A secondary goal was to evaluate the influence of the combination of different CT parameter values, such as the product of tube current and beam time (mAs), pitch and equipment's rotation time, and their influence on the volumetric CT dose index (CTDI_{vol}), which is used as a reference index dose in CT examination. And lastly, to examine imaging quality parameters such as noise, CT number uniformity, accuracy, spatial resolution and figure of merit (FOM), for each suggested protocol to define the best one among the options.

2 Materials and Methods

This study was developed at CHC-UFPR Diagnostic Imaging Unit using a Philips MX 16-Slice CT scan (Koninklijke Philips N.V., Eindhoven, Netherlands) (see Fig. 1).

The evaluation of the suggested protocols was based on a comparison between five different exposures made in the head phantom simulator (see Fig. 2), changing operational parameters for each one.

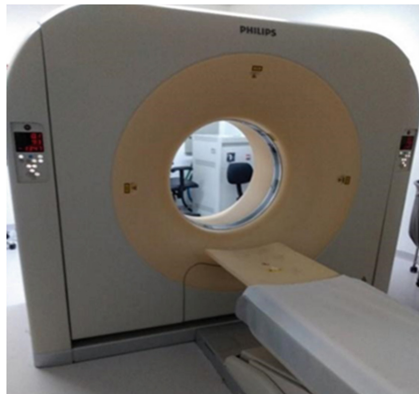


Fig. 1. MX 16-Slice scanner by Philips at the CHC-UFPR. Its x-ray tube contains a maximum capacity of 140 kV with an operating current of 355 mA for that voltage, and maximum output power of 50 kW.

The quality assurance tests were made by analyzing sliced images of two out of the three layers the simulator possesses. Firstly the "Water layer" for the evaluation of noise level, FOM, CT number uniformity, and accuracy. Secondly and lastly, the images of the multi-pin layer of the phantom were considered for evaluating special resolution.



Fig. 2. Head-16 Simulator used in daily MX 16 scanner's quality tests at the CHC-UFPR.

To avoid unnecessary exposures, patient dose values for each protocol parameter set were simulated on the impactscore.org website, where it is possible to calculate, according to the manufacturer and scan model, all the patient dosimetry together with exposure factors.

Although it demonstrates how to change the parameters to minimize the CTDIvol, this simulation could not be used to compare the values obtained in the CT's adult skull test acquisitions directly, because it only shows a theoretical value available on their database. Since the website's database did not have the same equipment as the one used in this study, the Philips Brilliance 16 model was used in the simulation, as it contains a similar configuration to the CHC-UFPR equipment, only as a base to choose which parameters would be changed on the real protocol suggestions. Table 1 presents the CTDIvol values simulated by ImpactScan in each suggestion.

Table 1. Brilliance-16 CTDIvol simulated values obtained using ImpactScan.org.

Protocol	Simulated CTDIvol (mGy)	Real CTDIvol (mGy)
Routine	46.8	46.25
1	43.7	–
2	43.6	–
3	40.4	–
4	43.6	–

It is worth mentioning that the simulation parameter values are not the same as those acquired in the real tests, because Philips CT scans have pre-established values of mAs, pitch and rotation time that cannot be changed manually, only selected from a list. Therefore, the values presented on Table 2 are not the same used on the ImpactScan simulation because they vary from one scan to another.

Aside from routine acquisition protocol, the other four suggested exposures with the Head-16 simulator were done by using different operation parameter values (see Table 2) to evaluate dose optimization and image quality conditions.

These parameters: operation current by effective time product, as well as pitch and tube's rotation time were changed, whilst maintaining the same high voltage tube for each one of them.

Table 2. Operational parameter values for each suggested protocol acquired with the MX 16-Slice scanner.

Protocol	High voltage tube (kV)	Product of operating current by time (mAs)	Pitch	Rotation time (s)
Routine	120	300	0.6713	0.75
1	120	280	0.6713	0.60
2	120	280	0.6042	0.60
3	120	260	0.5035	0.60
4	120	280	0.5035	0.75

The image analysis was made using the ImageJ software (see Fig. 3), which allows calculating the mean and standard deviation of regions of interest (ROIs) delimited in each measurement performed.

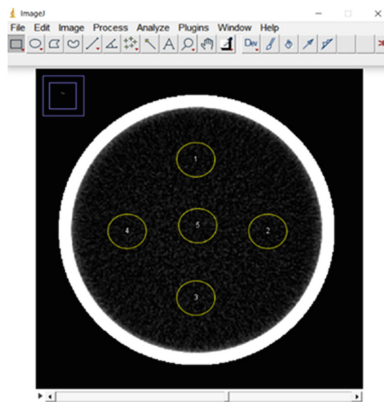


Fig. 3. ImageJ software with a CT image containing 5 circular ROIs, acquired from the head simulator's water layer.

2.1 Spatial Resolution

Following the manufacturer's instructions, the evaluation of the spatial resolution was performed by using the image 'cut' referring to the multi-pin layer of the Head-16

simulator (see Fig. 2). In this layer, there is an arrangement of 7 rows, each with a set of 5 pins of different thicknesses, spaced differently where row number 1 has the smallest space between the pins and row 7 the largest. The criterion was that all pins should be visible in the CT image.

To maintain a standard in image visualization and reliability in the visual analysis it was decided to use the ImageJ software for evaluating the image structures to minimize possible human eye mistakes. Profiles of each row of pins were plotted by arranging a linear ROI on top of the rows (see Fig. 4) so that the gray value of each could be measured.

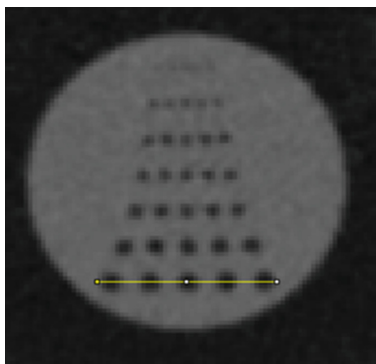


Fig. 4. CT Image showing the rows of pins with a linear ROI positioned on the 7th row, acquired from the multi-pin layer used for the evaluation of spatial resolution.

The plots had a wave pattern where the valleys represented the pins and the crests the spacing between them. In the plot, 5 valleys should be visualized (see Fig. 5).

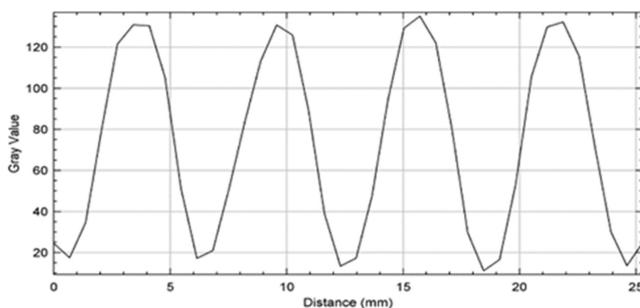


Fig. 5. Wave pattern on Gray Value versus Distance graph, plotted using the ImageJ software.

2.2 The Figure of Merit (FOM)

The FOM can be used as an image quality metric, since the higher it is, the lower the dose delivered to the patient will be. it was possible to compare the optimization between

the acquisition methods relating image quality parameters (such as spatial resolution or noise) with image acquisition parameters (such as slice thickness or dose). The equation is given by:

$$FOM = \frac{CNR^2}{CTDI_{VOL}} \quad (1)$$

where CNR is the contrast-to-noise ratio squared divided by the value of CTDI_{VOL} of each protocol suggested and used in the routine of CHC-UFPR.

CTDI_{VOL}'s value was obtained from the dose description of each protocol and the CNR was defined by subtracting the mean numerical signal of the background region of the image and the mean signal referring to the image object, divided by the standard deviation of the background signal as the following equation:

$$CNR = \frac{S_F - S_O}{\sigma} \quad (2)$$

with S_F being the mean signal of the background region of the image, S_O being the mean signal referring to the image object and σ the standard deviation of the background signal.

2.3 Noise Level (N)

Noise level (N) was estimated by dividing the value of the standard deviation (σ) of the central ROI on the water layer of the simulator by the difference between water and air's CT numbers (approximately 1000), multiplied by 100%, as the equation:

$$N = \frac{\sigma_{ROI}}{1000} \times 100\% \quad (3)$$

According to IN 93, the CT image's noise tolerance must be less than, or equal to 15% added to the reference value used in the QC test.

2.4 CT Number's Accuracy and Uniformity

To perform the CT number's uniformity and accuracy tests 5 ROIs were positioned in the water layer image to analyze the mean signal in these regions. One ROI is in the central zone and the other four are in peripheral regions of the slice, corresponding to 3, 6, 9 and 12 o'clock positions (Fig. 3).

Accuracy (ΔCT) was calculated by the difference between the value of the CT number measured in the central ROI and the nominal CT value, this being zero for water and 1000 for air as shown in the equation:

$$\Delta CT = CT_C - CT_{NOM} \quad (4)$$

where CT_C is the CT number in the central region and CT_{NOM} being the nominal CT number for water.

Uniformity (U) was calculated by subtracting the peripheral CT number (CTP) and the central CT number (CTC), both corresponding to the signal measured in the image's placed ROI as the equation follows:

$$U = CT_P - CT_C \quad (5)$$

The values of CT numbers tolerance limits for accuracy and uniformity, following IN 93 were (0 ± 5) HU (for water), and ≤ 5 HU, respectively.

3 Results and Discussion

3.1 Spatial Resolution

The plot of the profiles of the first row of pins for all the protocols studied is shown in Fig. 6. In it, it is possible to observe the five valleys, although poorly defined, for all the protocols studied, except for the routine protocol. The protocols with better visualization of the valleys in the profiles were protocols 1 (red), 2 (light green), and 3 (dark blue).

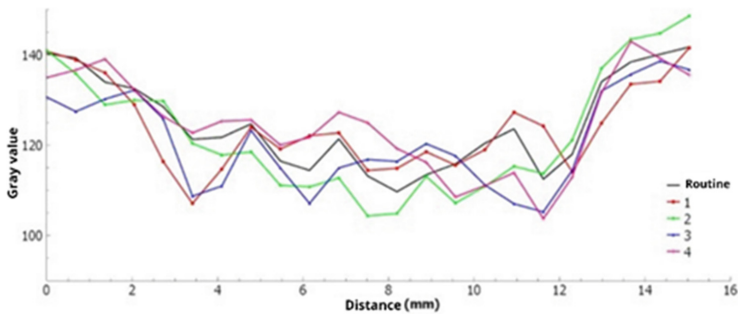


Fig. 6. Comparison between the plotted profiles using the 1st row for each protocol.

In row number 7 (see Fig. 7) it was possible to identify each of the pins in all the suggested protocols, including the routine protocol, as recommended in the instruction manual of the phantom.

It is worth mentioning that row 1 has the smallest pins with the smallest spacing between them, while row 7 has the biggest pins with the biggest spacings. In this way, better visualization of the wave pattern is expected in the plot of the profiles of row number 7.

3.2 The Figure of Merit (FOM)

As the aim was to obtain the highest possible FOM, it was analyzed that all acquisitions, except for number 4, had a higher FOM than the reference protocol, as shown in Table 3, as well as the CTDIVOL values obtained in each acquisition.

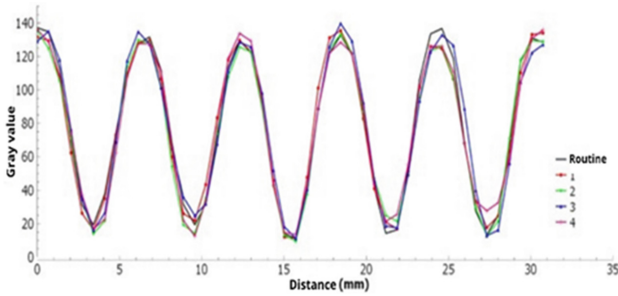


Fig. 7. Comparison between the plotted profiles using the 7th row for each protocol.

Table 3. CTDIvol and FOM comparison between all suggested protocols.

Protocol	NCR	CTDIvol (mGy)	FOM
Routine	27.80	46.25	16.71
1	28.80	43.21	19.18
2	31.01	43.11	22.31
3	26.53	40.09	17.55
4	26.33	43.29	16.01

3.3 Noise Level (N) and CT Number's Accuracy and Uniformity

For the noise level test, following IN 93, the variation value regarding the reference level should not exceed 15%. Therefore, using the routine protocol as a baseline, the noise level would have to be less than or equal to 4.513, or less than 0.45%.

All acquisitions obtained noise levels within the recommendations. As the parameters in each suggested protocol were designed to reduce the CTDIvol, a small increase in the noise level was already expected concerning the protocol used in the routine, because the lower the dose value, the higher the level of noise. Noise in the image. It was observed that protocol 3 exceeds the tolerance value and that lower levels were obtained with suggested protocols 1 and 4.

Regarding the uniformity of the CT number, also following IN 93, the value of deviation from the reference value should be less than or equal to ± 5 HU. It is worth mentioning that the deviations in the uniformity value of all acquisitions were minimal and did not reach 0.4 HU.

In the evaluation of the CT number's accuracy, all values found were within the recommendations for evaluation in the water of (0 ± 5) HU, according to IN 93. All results are shown in Table 4.

It was noted that acquisition 3, in the accuracy assessment, was the closest to the tolerance value of 5 HU and that protocols 1 and 4 had the smallest accuracy variation compared to the routine.

Table 4. Noise, uniformity and accuracy test results for each acquired protocol.

Protocol	σ ROI	Noise level (%)	Uniformity (HU)	Accuracy (HU)
Routine	3.925	0.39	-0.174	3.925
1	4.151	0.42	-0.057	4.151
2	4.354	0.44	-0.322	4.354
3	4.537	0.45	-0.385	4.537
4	4.179	0.42	-0.331	4.179

Thus, among the evaluated protocols, numbers 3 and 4 were outside the acceptance criteria, while protocols 1 and 2 were compliant in all proposed quality tests, as shown in Table 5.

Table 5. Performed tests' List containing the acceptance criteria for each parameter and results for each protocol acquired.

Parameters	Acceptance criteria	Routine (reference protocol)	1	2	3	4
Spatial resolution	To visualize five peaks in the plot (manufacturer's recommendation)	✓ ¹	✓	✓	✓	✓
FOM	Higher than, or equal to the reference number	✓	✓	✓	✓	×
Noise	≤15% above the reference value	✓	✓	✓	×	✓
Accuracy	0 ± 5 (water)	✓	✓	✓	✓	✓
Uniformity	≤5 HU	✓	✓	✓	✓	✓

Table 6 shows the comparison of the quality parameters between the routine protocol and the suggestions for protocols 1 and 2. Observing the values in the table, it is noted that protocol 1 presented noise, uniformity, and accuracy values closer to the values obtained with the routine protocol when compared to protocol 2.

However, the acquisition with protocol 2 also brings a reduction in the value of CTDIVOL and a greater increase in FOM, that is, better image quality is obtained with an optimization of the dose. Therefore, considering the acceptance criteria for image quality in CT scans, within all protocols, only numbers 1 and 2 showed satisfactory results.

In addition, with these two protocols, a reduction in CTDIVOL of approximately 6.5% was obtained, and an increase of an average of 28.2% in FOM concerning the protocol already used in the routine.

¹ "✓" for compliant and "×" for non-compliant.

Table 6. Results comparison between routine's reference values and the acquired protocols 1 and 2.

Parameters	Reference value	Protocol 1	Protocol 2
CTDI _{vol} (mGy)	46.25	43.21	43.11
FOM	16.71	19.18	22.31
Noise (%)	0.39	0.42	0.44
Uniformity (HU)	-0.174	-0.057	-0.322
Accuracy (HU)	3.925	4.151	4.354

4 Conclusions

In this study, the CT Contrast-free adult skull protocol was optimized by changing some acquisition parameters such as rotation time, pitch, and tube current product by beam time, to reduce the CTDI_{vol} value, maintaining the image quality.

In all protocols proposed, a significant reduction in the value of CTDI_{vol} was observed due to the change in the value of the current product of operation by time, from 300 to 280 mAs.

Thus, it is suggested that UDIM carry out an analysis of the images acquired with protocols 1 and 2 together with radiologists to compare the quality of the images because, in addition to the quantitative evaluation of the parameters, a qualitative evaluation is also necessary to enable the establishment of a new protocol that best fits the physician's criteria for the hospital's medical report.

References

1. Seeram, E.: Studyguide for Computed Tomography: Physical Principles, Clinical Applications, and Quality Control, 4th edn. Saunders, United States (2015)
2. Tauhata, L., Salati, I., Di Prinzio, R., Di Prinzio, A.: Radioproteção e Dosimetria: Fundamentos, 10th edn. IRD/CNEN, Rio de Janeiro (2014)
3. Samei, E., Bakalyar, D., Boedeker, K. L., et al.: Performance Evaluation of Computed Tomography Systems. In: AAPM Task Group 233 Report, pp 1–71. American Association of Physicists in Medicine, United States (2019)
4. International Atomic Energy Agency.: Quality Assurance Programme for Computed Tomography: Diagnostic and Therapy applications. In: IAEA Human Health Series, Austria (2012)
5. Agência Nacional de Vigilância Sanitária.: Radiodiagnóstico Médico: Desempenho De Equipamentos e Segurança. 1st ed. Editora Anvisa, Brasília (2005)
6. Agência Nacional de Vigilância Sanitária.: RDC 611: Instrução Normativa No 93. Ministério da Saúde, Brasília (2022)
7. Rehani, M. M.: ICRP and IAEA Actions on Radiation Protection in Computed Tomography. In: Annals of the ICRP, vol. 41, pp. 154–160. IAEA, Austria (2012)